Bull. Chem. Soc. Jpn., **77**, 1297–1303 (2004)

Transport Properties and Effective Intermolecular Potentials for O_2–O_2, N_2–N_2, and O_2–N_2

Ali Maghari* and Amir Hossein Jalili

Department of Chemistry, University of Tehran, Tehran, Iran

Received November 4, 2003; E-mail: maghari@khayam.ut.ac.ir

Effective intermolecular potential-energy functions for O_2–O_2, N_2–N_2, and O_2–N_2 are obtained directly from the extended law of corresponding states for viscosity and experimental second virial coefficient data. The results are then used to obtain a best Morse–Spline–van der Waals (MSV) potential model. The present potential functions provide the best overall agreement for the available low-density gas-phase thermophysical data, i.e., second virial coefficient and transport properties. The effective intermolecular potential energies from the inversion of thermophysical data reproduce the viscosity, diffusion coefficient, and other transport coefficients within the experimental accuracy.

Over the past three decades, the determination of an accurate interaction potential energy has been an area of vigorous activity. The intermolecular pair potential has been shown to reproduce many of the bulk properties of matter, such as the second virial coefficient and transport properties.[1–6] Several procedures, including the analysis of molecular-beam scattering data,[7–9] multiproperty fits[10] and ab initio calculation methods,[11–13] have been utilized in order to arrive at quantitative representations of the interaction potential energies for such systems.

A numerical method for the direct inversion of measured transport coefficients and second virial coefficient to find the intermolecular potential energy, without any explicit assumption about the functional form of the potential, has been developed by E. B. Smith and co-workers.[14–18] The inversion procedure turned out to be quite successful, since by no other method can one directly determine a unique potential function from the inversions of a set of experimental data. If we can obtain such information from one property, then we may be able to calculate another useful property of the gas and thereby relieve ourselves of the need to measure it.

For monatomic systems, the direct inversion technique can give an accurate intermolecular potential energy. This algorithm for polyatomic systems permits us to generate centrally symmetrical effective interaction potential energy. Such a potential is then used to computable of the other fluid transport properties. The method used in this work was an iterative one, and converged rapidly once a good choice had been made for the initial starting potential.

The effective interaction potential energies of nitrogen, oxygen and their mixture are important for many studies. In particular, they are needed to determine certain input data required for a real gas analysis of aerodynamic flows. Knowledge of the properties of the N_2/O_2 mixture is important for understanding upper-atmosphere chemistry and atmospheric reentry.

In this paper we perform a direct inversion method to determine the inner branch of the effective potential energy of pairs of O_2–O_2, N_2–N_2, and O_2–N_2 corresponding to the experimental viscosity collision integral and the outer branch of their effective interacting potential energy, corresponding to the second virial coefficient data. The obtained results are fitted to a multiparameter MSV (Morse–Spline–van der Waals) potential model. The effective intermolecular potential energies from the inversion of thermophysical data reproduce the viscosities, diffusion coefficients, and other transport coefficients within the experimental accuracy.

Effective Pair Potential from Thermophysical Data

According to the kinetic theory of gases at low-densities and the Chapman–Enskog solution[19] of the Boltzmann transport equation, the transport properties can be expressed based on a series of collision integrals that depend on the intermolecular potential energy, which is defined as

$$\theta = \pi - 2b \int_{r_0}^{\infty} \frac{r^{-2}\mathrm{d}r}{\{1 - (b^2/r^2) - [U(r)/E]\}^{1/2}}, \tag{1}$$

$$Q^{(l)}(E) = 2\pi \left[1 - \frac{1 + (-1)^l}{2(1 + l)} \right]^{-1} \int_0^{\infty} (1 - \cos^l \theta) b \mathrm{d}b, \tag{2}$$

$$\begin{aligned}\Omega^{(l,s)}(T) &= [(s+1)!(k_\mathrm{B}T)^{s+2}]^{-1} \\ &\quad \times \int_0^{\infty} Q^{(l)}(E) \exp\left(\frac{-E}{k_\mathrm{B}T}\right) E^{s+1}/\mathrm{d}E,\end{aligned} \tag{3}$$

where θ is the scattering angle, $Q^{(l)}(E)$ is the transport collision integral, b is the impact parameter, E is the relative kinetic energy of colliding molecules, $U(r)$ is the potential energy, r is the radial coordinate, and r_0 is the closest approach of two molecules. Superscripts l and s appearing in the collision integral (Ω) denote weighting factors that account for the mechanism of transport by molecular collision. For example, for the two transport properties, viscosity and diffusion, the superscripts assume values of $l = 2$, $s = 2$ and $l = 1$, $s = 1$, respectively. Thus, three successive numerical integrations are required to obtain the collision integrals.

The Chapman–Enskog kinetic theory[19] of a single dilute monatomic or spherical gas leads to the expression

Published on the web July 9, 2004; DOI 10.1246/bcsj.77.1297

$$\eta(T)\,\frac{5}{16\sigma^2}\,[(mk_{\mathrm{B}}T/\pi)^{1/2}/\Omega^{(2,2)*}(T^*)]f_\eta, \tag{4}$$

for the viscosity η of a pure gas at temperature T, where $\Omega^{(2,2)*}(T^*)$ is the reduced viscosity collision integral as a function of the reduced temperature, $T^* \equiv k_{\mathrm{B}}T/\mathcal{E}$ and m is the mass of the molecule. Here, k_{B} is Boltzmann's constant and f_η is a correction factor that depends slightly upon the temperature and the interaction potential, but which seldom deviates from unity by more than 1%. In this equation, the reduced collision integral ($\Omega^{(2,2)*}$) may be defined as

$$\Omega^{(2,2)*} = \frac{\Omega^{(2,2)}}{\pi\sigma^2}\,. \tag{5}$$

For non-spherical polyatomic molecules, however, the theory is complicated, caused by anisotropic forces associated with the internal structures of the molecule. In particular, the kinetic theory of polyatomic molecules, which takes into account inelastic collisions, is extremely complex and there have been only a few, approximate attempt to calculate the transport properties from this theory. In order to make numerical calculation for the transport properties of polyatomic molecules, a simple approximation has been proposed by Monchick and Mason, who assumes that the Chapman–Enskog theory of non-spherical molecules retains its original form, but the collision integrals must be averaged over all possible relative orientations occurring in collisions.[20] Their classical model ignores inelastic collisions, thus restricting its applicability to viscosity and diffusion coefficients, and also to the translational part of thermal conductivity (frozen thermal conductivity). The collision integrals can then be calculated assuming that molecules collide with a fixed relative orientation during encounters. Therefore, the transport properties are determined by the collision integrals averaged over all of the initial orientations. Thus, the Monchick–Mason collision integral, which is used in our calculation, is given by

$$\langle\Omega^{(2,2)*}(T^*)\rangle = \frac{1}{\pi}\int_0^{\pi}\int_0^{1}\int_0^{1}\Omega^{(2,2)*}\mathrm{d}\varphi\mathrm{d}(\cos\theta_1)\mathrm{d}(\cos\theta_2), \tag{6}$$

where $\langle\Omega^{(2,2)*}(T^*)\rangle$ is an orientation-averaged reduced viscosity collision integral.

The physical basis for the Monchick–Mason assumption is that most of the interaction in a collision occurs in the vicinity of the distance of closest approach, during which the relative orientation does not change much, so that one relative orientation dominants each collision. The expression for a typical interaction viscosity coefficient, $[\eta_{12}]_1$, of a gas mixture is the same as Eq. 4 for a single gas with $f_\eta = 1$ and m replaced by $m_{12} = 2m_1m_2/(m_1 + m_2)$,

$$[\eta_{12}]_1 = \frac{5}{16}\left(\frac{5m_1m_2k_{\mathrm{B}}T}{(m_1+m_2)\pi}\right)^{1/2}\frac{1}{\sigma_{12}^2\langle\Omega_{12}^{(2,2)*}(T_{12}^*)\rangle}, \tag{7}$$

where subscripts 1 and 2 denote the different pure components. Experimental values of $[\eta_{12}]_1$ can be extracted from measurements of the whole mixture as a function of the composition.[21]

The measured $\eta(T)$ for a dilute gas can be inverted by the method described in the following paragraph to yield the reduced centrally symmetrical effective interaction potential, $U^*(r^*) \equiv U/\mathcal{E}$, as a function of the reduced distance, $r^* \equiv r/\sigma$, in which σ is a distance scaling parameter, such that $U(\sigma) = 0$, and $\mathcal{E}$ is the depth of the potential well. A precisely accurate correlation formula for the low-density transport properties of nitrogen, oxygen and its mixture was proposed by Bzowski and co-workers over a wide temperature range.[22,23] The orientational average reduced collision integral, $\langle\Omega^{(2,2)*}(T^*)\rangle$, for the viscosities of N_2–N_2, O_2–O_2, and N_2–O_2 is thus related to the reduced temperature (T^*) as

$$\begin{aligned}\langle\Omega^{(2,2)*}\rangle &= \exp[0.46641 - 0.56991(\ln T^*)\\ &\quad + 0.19591(\ln T^*)^2 - 0.03879(\ln T^*)^3\\ &\quad + 0.00259(\ln T^*)^4] \quad \text{for} \quad 1 \le T^* \le 10,\end{aligned} \tag{8a}$$

$$\begin{aligned}\langle\Omega^{(2,2)*}\rangle &= \rho^{*2}\alpha^2\lfloor 1.04 + a_1(\ln T^*)^{-1}\\ &\quad + a_2(\ln T^*)^{-2} + a_3(\ln T^*)^{-3}\\ &\quad + a_4(\ln T^*)^{-4}\rfloor \quad \text{for} \quad T^* \ge 10,\end{aligned} \tag{8b}$$

where $\langle\ldots\rangle$ denotes the angle average of the collision integral and the values of ρ^*, α, and a's were previously define.[22] An expression for $\langle\Omega^{(2,2)*}(T^*)\rangle$ in the low-temperature region ($T^* < 1$) has not been obtained, because (i) no experimental information concerning viscosity at the low temperatures is available and (ii) the existence of several long-range contributions to the interaction potential, whose effects on the low-temperature properties can not be separated. The experimental viscosity data used in this work covered the temperature range of about 110–2100 K.

For the sake of simplicity, we use $\Omega^{(l,s)*}$ instead of $\langle\Omega^{(l,s)*}\rangle$ in later expressions.

Inversion Scheme. The direct inversion procedure of Smith and co-workers[15–18] is based on the idea that at a given temperature T, there is a separation distance r at which the potential U is approximately equal to $k_{\mathrm{B}}T$ and the viscosity collision integral $\Omega^{(2,2)}$ is approximately equal to πr^2. It is always possible for a given intermolecular potential to find a function $G^\eta(T^*)$ for which this idea becomes exact through the equations

$$r = \sqrt{\Omega^{(2,2)}/\pi}, \tag{9}$$

$$U_n(r) = k_{\mathrm{B}}TG_n^\eta(T^*), \tag{10}$$

where $G_n^\eta(T^*)$ is the n'th inversion function and the subscript n refers to the n'th iteration number. Eqs. 9 and 10 are central equations in the inversion scheme.

The inversion technique begins by employing the experimental viscosity collision integral from corresponding states correlation equations given by Bzowski et al.[22,23] [Eqs. 8a and 8b] to convert data points ($\Omega_{\mathrm{exp}}^{(2,2)*}$, T^*) to their corresponding ($U^* \equiv U/\mathcal{E}$, $r^* \equiv r/\sigma$) on the potential energy curve. We then make an initial guess of G^η from an initial model potential energy function, denoted by $U_0(r)$. A reasonable choice for this initial approximation is the Lennard-Jones (12, 6) model, where the values of $\Omega^{(2,2)*}(T^*)$ of this model potential are given by Viehland et al.[24] From this initial-guessed potential function, we generate the inversion function ($G_0^\eta(T^*)$)

$$G_0^\eta(T^*) = U_0^*(r_0^*)/T^*, \tag{11}$$

where subscript 0 denotes that G^η corresponds to the initial estimate of the potential.

The fundamental postulate of the inversion procedure is then that the series of data points (U_1, r) generated by applying

$$r = \sqrt{\Omega_{\text{exp}}^{(2,2)}/\pi}, \tag{12}$$

$$U_1 = k_B T G_0^{\eta}(T^*), \tag{13}$$

to the experimental data at each temperature, constitute a closer approximation to the true potential than does the origin, guessed, function, $U_0(r)$. To develop an iterative scheme it is therefore necessary to extrapolate the function $U_1(r)$ to both larger and smaller separations in order that its collision integrals, $\Omega_1^{(2,2)*}$, can be computed. At long range this extrapolation may be performed by means of one inverse sixth-power function,

$$U(r) = -\frac{C_6}{r^6} \quad \text{as} \quad r \to \infty, \tag{14}$$

which is known to be the true asymptotic limit, where C_6 is the dispersion coefficient. It is remarkable to mention that the inversion procedure is insensitive to the nature of the extrapolating function.[15]

Once these extrapolations have been carried out, the first iterate potential ($U_1(r)$) may be employed to compute its corresponding collision integrals ($\Omega_1^{(2,2)*}$) using Eqs. 1–3, and hence a new inversion function through equations similar to aforementioned equation:

$$r_1^* = \sqrt{\Omega_1^{(2,2)*}}, \tag{15}$$

$$G_1^{\eta}(T^*) = U_1^*(r_1^*)/T^*. \tag{16}$$

The triple integrals 1–3 are evaluated by using the Gatland version of a computer program developed by O'Hara and Smith.[25,26] This new inversion function can then be used to generate a second iterate sequence of data points (U_2, r) for the true potential by repeated use of Eqs. 9 and 10:

$$r^* = \sqrt{\Omega_{\text{exp}}^{(2,2)*}}, \tag{17}$$

$$U_2 = k_B T G_1^{\eta}. \tag{18}$$

The new potential is a closer approximation to the true potential energy than the potential of the initial model, and thus the process may be repeated until convergence occurs. It must be mentioned that the $\Omega_{\text{exp}}^{(2,2)*}$ values are obtained from the correlation equations 8a and 8b.

The present results converged after three iterations. The viscosity data, which has been used to invert the centrally symmetrical effective interaction potential energy for N_2–N_2, O_2–O_2, and N_2–O_2, provide us only with the potential at distance $r^* \leq$ 1.3 Furthermore, it can be shown that the negative potential well is only partly determined, in that its width can be found as a function of its depth.[27] However, knowing the inner branch of the potential well ($r^* \leq 1.3$) from the viscosity (Eq. 17), we can use this information in conjunction with the second virial coefficient data to determine the outer branch (attractive region) of the well uniquely, so we have

$$U^* = T^* - 1, \tag{19}$$

$$r_R^* - r_L^* = -\frac{2\pi}{3} N_0 (B_2^* - 1) N(T^*), \tag{20}$$

where r_R^* and r_L^* are the reduced coordinates of the outer and inner walls of the potential well, respectively, N_0 is Avogadro's number, $N(T^*)$ is a function of T^*, whose numerical values are tabulated by Clancy et al.,[27] and $B_2^* \equiv 3B_2/2\pi N_0 \sigma^3$ is the reduced second virial coefficient, where B_2 is the second virial coefficient. Knowing the inner branch of the potential well from the viscosity, we can use this information in conjunction with the second virial coefficient data to uniquely determine the outer branch of the well. The selection of the experimental second virial coefficient data was guided by critical survey by Dymond and Smith[28] and the present work of Hall.[29]

Results and Discussion

The effective interaction potential energies for O_2–O_2, N_2–N_2, and N_2–O_2 have been determined by using a direct inversion of the experimental correlation of the viscosity data. Eqs. 9 and 10 define the coordinates of a point (U^*, r^*) on the effective intermolecular pair potential curve. It should be mentioned that the viscosity collision integrals for a polyatomic molecular gas at low temperature are not available, and therefore our effort was just devoted to a calculation for which $T^* \geq 1$. At long range, only the well-width of the potential obtained from the second virial coefficient data is available. This has been used in conjunction with the inner coordinates of the well obtained in the viscosity inversion to give the effective potential energy in the separation range.

The obtained results are fitted in the usual way by assuming a multiparameter potential form. The parametric potential form chosen is the Morse–Spline–van der Waals (MSV) piecewise function with the following form:

$$U^*(r^*) = \exp[2\beta(1 - \gamma r^*)] - 2\exp[\beta(1 - \gamma r^*)] \qquad r^* \leq r_1^*, \tag{21a}$$

$$= b_1 + (r^* - r_1^*)\{b_2 + (r^* - r_2^*)[b_3 + (r^* - r_1^*)b_4]\} \qquad r_1^* < r^* \leq r_2^*, \tag{21b}$$

$$= -C_6^*/r^{*^6} \qquad r_2^* < r^* \leq \infty, \tag{21c}$$

where $C_6^* \equiv C_6/\varepsilon\sigma^6$ is a long-range dimensionless constant, and $\gamma \equiv \sigma/r_m$, where r_m is the distance at the location of the attractive minimum. A Morse function and the van der Waals dispersion expansion are used for the well and long-range interactions, respectively. The spline function is also used for joining them smoothly. Parameters that provide the best fit to the inversion data are given in Table 1. The values of the scaling potential parameters, σ and ε/k_B, can be obtained from the experimental viscosity data at two arbitrary temperatures, T_1 and T_2. For this purpose, we can first define the quantity K_η by

$$K_\eta = \left[\frac{\eta(T_2)}{\eta(T_1)}\right]_{\text{exp}} \left(\frac{T_1}{T_2}\right)^{1/2}. \tag{22}$$

Using Eq. 4, we can obtain an alternative equation in terms of T^*

$$K_\eta = \left[\frac{\Omega^{(2,2)*}(T_1^*)}{\Omega^{(2,2)*}(T_2^*)}\right]\left[\frac{f_\eta(T_2^*)}{f_\eta(T_1^*)}\right], \tag{23}$$

where the reduced temperature (T_i^*) relates to ε/k_B as

$$T_i^* = \frac{k_B T_i}{\mathcal{E}}. \tag{24}$$

Here, the higher-order correction factor, $f_\eta(T^*)$, is

$$f_\eta = 1 + \frac{3}{196}(6E^* - 7)^2, \tag{25}$$

which seldom deviates from unity by more than 1%. By employing the experimental points of (η, T), the experimental value of K_η can be obtained from Eq. 22. Making an initial guess at the potential well depth that denotes it by $\mathcal{E}_0$, the initial estimates of data points ($\Omega^{(2,2)*}$, T^*) and (f_η, T^*) may be obtained at two temperatures, T_1 and T_2, by applying Eqs. 23 and 24 and Tables 2–4. As a first approximation to $\mathcal{E}/k_B$ we may use the value calculated from the critical temperature[21] as $\mathcal{E}_0/k_B = 0.77T_c$, where T_c is the critical temperature. We then generate the approximate value of K_η from Eq. 23 and compare it with the observed value of K_η obtained from Eq. 22. We used repeated trials to establish the minimum deviation between the observed value of $\mathcal{E}/k_B$, based on Eq. 22, and the calculated value of $\mathcal{E}/k_B$, obtained from Eq. 23. Once the value of $\mathcal{E}/k_B$ has been determined, the parameter is obtained from the equation

$$\sigma = \left\{ \frac{266.93\sqrt{mT_i}\, f_\eta(T_i^*)}{[\eta(T_i) \times 10^7]\Omega^{(2,2)*}(T_i^*)} \right\}^{1/2}, \tag{26}$$

in which T_i is either T_1 or T_2. The parameter C_6^* was also estimated from the last data point in the attraction region, $U^*(r^*) = -C_6^*/r^{*^6}$. The values of the scaling potential parameters (σ, $\mathcal{E}/k_B$, and C_6^*) obtained in this work are given in Table 1.

Table 1. The MSV Potential Parameters

Potential parameters	N_2–N_2	O_2–O_2	N_2–O_2
σ/Å	3.656	3.418	3.537
$\mathcal{E}/k_B$ (K)	96.8	118.8	106.7
β	6.521	6.663	6.576
$\gamma = \sigma/r_m$	0.894	0.897	0.895
r_1^*	1.188	1.188	1.188
r_2^*	1.636	1.636	1.611
b_1	−0.8889	−0.8731	−0.8828
b_2	1.5004	1.4161	1.5310
b_3	−2.4354	−2.9612	−2.6489
b_4	1.91923	3.9155	2.6007
$C_6^* \equiv C_6/\mathcal{E}\sigma^6$	4.154	4.413	4.111

The inverted reduced centrally effective potentials for O_2–O_2, N_2–N_2, and N_2–O_2 are shown in Fig. 1. Our obtained MSV centrally effective potential energy functions of O_2–O_2, N_2–N_2, and N_2–O_2 are also shown in Fig. 2. Note, however, from Fig. 2 and a comparison of the potential-well parameters given in Table 1, one can conclude that the O_2–O_2 potential is much more attractive at small r. The N_2–N_2 potential, which is slightly deeper in the long-range van der Waals tail than the O_2–O_2 potential, is expected to yield a stronger bound state.

The obtained effective intermolecular potential energies from the inversion of thermophysical (viscosity and second virial coefficients) data reproduce the collision integrals and their ratios, which are needed to calculate other transport properties more accurately. The ratios of the collision integrals are found according to the following formulas:

$$A^* \equiv \frac{\Omega^{(2,2)*}}{\Omega^{(1,1)*}}, \tag{27a}$$

$$B^* \equiv \frac{5\Omega^{(1,2)*} - 4\Omega^{(1,3)*}}{\Omega^{(1,1)*}}, \tag{27b}$$

$$C^* \equiv \frac{\Omega^{(1,2)*}}{\Omega^{(1,1)*}}, \tag{27c}$$

Table 2. Dimensionless Collision Integrals and the Related Ratios for Oxygen

$\log T^*$	$\Omega^{(2,2)*}$	A^*	B^*	C^*	E^*	F^*
0.0	1.5853	1.1124	1.2023	0.8420	0.8761	0.9158
0.1	1.4193	1.1068	1.1718	0.8533	0.8846	0.9230
0.2	1.2834	1.1023	1.1471	0.8676	0.8972	0.9332
0.3	1.1749	1.1001	1.1291	0.8826	0.9110	0.9454
0.4	1.0890	1.1002	1.1165	0.8968	0.9237	0.9583
0.5	1.0201	1.1020	1.1078	0.9091	0.9340	0.9708
0.6	0.9635	1.1042	1.1014	0.9195	0.9418	0.9820
0.7	0.9158	1.1062	1.0963	0.9278	0.9476	0.9913
0.8	0.8746	1.1079	1.0930	0.9345	0.9524	0.9983
0.9	0.8389	1.1099	1.0929	0.9394	0.9571	1.0028
1.0	0.8081	1.1136	1.0969	0.9424	0.9615	1.0053
1.1	0.7811	1.1196	1.1038	0.9433	0.9642	1.0076
1.2	0.7557	1.1267	1.1092	0.9427	0.9635	1.0114
1.3	0.7294	1.1318	1.1079	0.9419	0.9590	1.0170
1.4	0.7004	1.1313	1.0975	0.9424	0.9529	1.0232
1.5	0.6691	1.1234	1.0795	0.9457	0.9481	1.0277
1.6	0.6372	1.1087	1.0578	0.9517	0.9467	1.0293
1.7	0.6073	1.0895	1.0367	0.9599	0.9498	1.0280
1.8	0.5815	1.0692	1.0191	0.9691	0.9565	1.0247
1.9	0.5609	1.0503	1.0061	0.9780	0.9653	1.0206
2.0	0.5456	1.0345	0.9976	0.9857	0.9746	1.0166

Table 3. Dimensionless Collision Integrals and the Related Ratios for Nitrogen

$\log T^*$	$\Omega^{(2,2)^*}$	A^*	B^*	C^*	E^*	F^*
0.0	1.5819	1.1099	1.1930	0.8451	0.8791	0.9170
0.1	1.4210	1.1052	1.1653	0.8573	0.8887	0.9251
0.2	1.2900	1.1019	1.1437	0.8716	0.9016	0.9357
0.3	1.1854	1.1010	1.1281	0.8861	0.9147	0.9481
0.4	1.1019	1.1020	1.1167	0.8994	0.9261	0.9611
0.5	1.0338	1.1039	1.1078	0.9110	0.9351	0.9737
0.6	0.9770	1.1055	1.1003	0.9208	0.9418	0.9848
0.7	0.9284	1.1063	1.0938	0.9291	0.9472	0.9937
0.8	0.8863	1.1064	1.0893	0.9360	0.9521	1.0000
0.9	0.8500	1.1071	1.0887	0.9412	0.9573	1.0036
1.0	0.8193	1.1099	1.0933	0.9444	0.9626	1.0053
1.1	0.7930	1.1159	1.1016	0.9453	0.9661	1.0069
1.2	0.7688	1.1238	1.1087	0.9443	0.9657	1.0103
1.3	0.7434	1.1300	1.1090	0.9429	0.9610	1.0159
1.4	0.7150	1.1307	1.0997	0.9428	0.9543	1.0223
1.5	0.6836	1.1239	1.0821	0.9454	0.9487	1.0272
1.6	0.6513	1.1099	1.0603	0.9511	0.9468	1.0291
1.7	0.6206	1.0911	1.0387	0.9591	0.9493	1.0279
1.8	0.5939	1.0707	1.0206	0.9682	0.9558	1.0247
1.9	0.5725	1.0517	1.0007	0.9772	0.9645	1.0207
2.0	0.5565	1.0356	0.9983	0.9850	0.9738	1.0167

Table 4. Dimensionless Collision Integrals and the Related Ratios for Nitrogen–Oxygen

$\log T^*$	$\Omega_{12}^{(2,2)^*}$	A_{12}^*	B_{12}^*	C_{12}^*	E_{12}^*	F_{12}^*
0.0	1.5868	1.1144	1.2039	0.8415	0.8758	0.9165
0.1	1.4199	1.1086	1.1730	0.8526	0.8839	0.9236
0.2	1.2829	1.1038	1.1479	0.8668	0.8963	0.9338
0.3	1.1735	1.1012	1.1294	0.8820	0.9101	0.9459
0.4	1.0869	1.1010	1.1167	0.8963	0.9230	0.9585
0.5	1.0177	1.1026	1.1084	0.9087	0.9337	0.9707
0.6	0.9612	1.1052	1.1028	0.9190	0.9419	0.9816
0.7	0.9139	1.1080	1.0992	0.9271	0.9481	0.9907
0.8	0.8733	1.1110	1.0980	0.9332	0.9531	0.9974
0.9	0.8382	1.1151	1.1008	0.9373	0.9578	1.0016
1.0	0.8078	1.1215	1.1087	0.9390	0.9619	1.0041
1.1	0.7808	1.1308	1.1198	0.9383	0.9637	1.0067
1.2	0.7546	1.1413	1.1284	0.9359	0.9613	1.0111
1.3	0.7261	1.1491	1.1284	0.9333	0.9546	1.0176
1.4	0.6937	1.1500	1.1170	0.9327	0.9462	1.0244
1.5	0.6580	1.1419	1.0961	0.9355	0.9396	1.0293
1.6	0.6216	1.1255	1.0706	0.9420	0.9375	1.0309
1.7	0.5874	1.1037	1.0454	0.9514	0.9407	1.0294
1.8	0.5581	1.0804	1.0243	0.9621	0.9485	1.0258
1.9	0.5347	1.0586	1.0087	0.9727	0.9588	1.0215
2.0	0.5173	1.0404	0.9984	0.9820	0.9696	1.0174

$$E^* \equiv \frac{\Omega^{(2,3)^*}}{\Omega^{(2,2)^*}}, \tag{27d}$$

$$F^* \equiv \frac{\Omega^{(3,3)^*}}{\Omega^{(1,1)^*}}. \tag{27e}$$

Numerical values of $\Omega^{(2,2)^*}(T^*)$ and the defined ratios A^*, B^*, C^*, E^*, and F^* for O_2 and N_2 are given in Tables 2 and 3.

The kinetic theory of the polyatomic equation for the viscosity of a binary mixture is

$$\eta_{\mathrm{mix}} = \frac{1 + Z_\eta}{X_\eta + Y_\eta}, \tag{28}$$

where

$$X_\eta = \frac{x_1^2}{[\eta_1]_1} + \frac{2x_1x_2}{[\eta_{12}]_1} + \frac{x_2^2}{[\eta_2]_1}, \tag{29a}$$

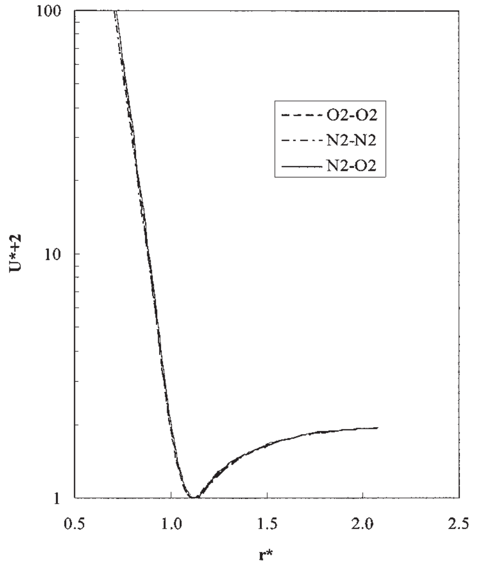

Fig. 1. Reduced pair potential obtained by INVERT of the corresponding state viscosity for O_2–O_2, N_2–N_2, and N_2–O_2. Note that the scale of reduced potential is logarithmic.

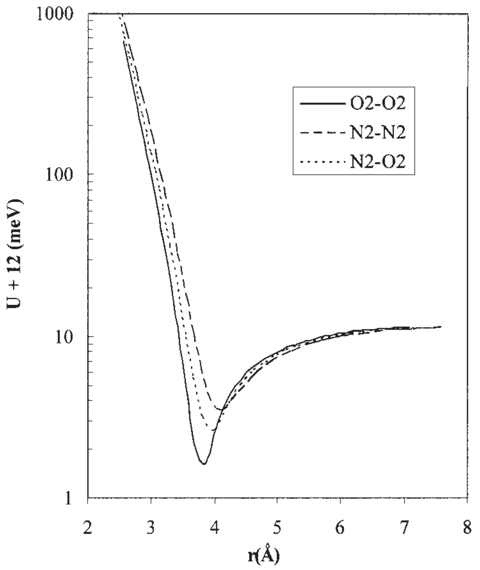

Fig. 2. The calculated Morse–Spline–van der Waals (MSV) intermolecular potential energy functions of the O_2–O_2, N_2–N_2, and N_2–O_2.

Table 5. Predicted Viscosities and Diffusion Coefficients from the Inversion Method and Absolute Average Percentage Deviations

T/K	O_2–O_2		N_2–N_2		N_2–O_2	
	$\eta/\mu\mathrm{Pa\,s}$	$10^4D/\mathrm{m^2\,s^{-1}}$	$\eta/\mu\mathrm{Pa\,s}$	$10^4D/\mathrm{m^2\,s^{-1}}$	$\eta^{a)}/\mu\mathrm{Pa\,s}$	$10^4D/\mathrm{m^2\,s^{-1}}$
150	11.17	0.0571	10.01	0.0584	10.46	0.0611
200	14.59	0.0989	12.92	0.1001	13.56	0.1044
250	17.73	0.1500	15.54	0.1505	16.37	0.1561
300	20.60	0.2092	17.93	0.2086	18.94	0.2153
400	25.75	0.3476	22.15	0.3440	23.72	0.3543
500	30.38	0.5140	25.82	0.5061	27.75	0.5183
600	34.62	0.7045	29.21	0.6917	31.64	0.7022
700	38.59	0.9174	32.71	0.8991	35.15	0.9097
800	42.31	1.2147	36.18	1.1897	38.45	1.2042
900	45.82	1.4735	39.11	1.4431	41.52	1.4608
1000	49.16	1.7514	41.90	1.7168	44.72	1.7370
AAD%	0.752	2.61	0.526	2.16	0.675	2.40

Absolute average percent deviation is defined as follows: AAD% $= (1/N)\sum_{i=1}^{N} Abs[(Calc_i - Expt_i)/Expt_i] \times 100$. a) The mole fraction of N_2 is 0.6216. Experimental data are taken from Ref. 30–43.

$$Y_\eta = \frac{3}{5}A^*_{12}\left\{\frac{x_1^2}{[\eta_1]_1}\left(\frac{m_1}{m_2}\right) + \frac{2x_1x_2}{[\eta_{12}]_1}\left[\frac{(m_1+m_2)^2}{4m_1m_2} \times \left(\frac{[\eta_{12}]_1^2}{[\eta_1]_1 + [\eta_2]_1}\right)\right] + \frac{x_2^2}{[\eta_2]_1}\left(\frac{m_2}{m_1}\right)\right\}, \tag{29b}$$

$$Z_\eta = \frac{3}{5}A^*_{12}\left\{x_1^2\left(\frac{m_1}{m_2}\right) + 2x_1x_2\left[\frac{(m_1+m_2)^2}{4m_1m_2} \times \left(\frac{[\eta_{12}]_1}{[\eta_1]_1} + \frac{[\eta_{12}]_1}{[\eta_2]_1}\right) - 1\right] + x_2^2\left(\frac{m_2}{m_1}\right)\right\}. \tag{29c}$$

Here, subscripts 1 and 2 denote the different pure components, A^*_{12} is the ratio of the binary collision integrals (Eq. 27a), $[\eta_{12}]_1$ is the interaction viscosity coefficient obtained from the Eq. 7 and x their mole fractions in the mixture. However, it has been demonstrated that, provided the experimental values of the pure gas viscosities are employed to replace the first-order approximation to them, $[\eta_i]_1$, no significant error results, especially for mixtures in which the species mass ratio is near to unity.

Moreover, the expression for the self diffusion (D_i) at a given pressure (P) is

$$D_i = \frac{3}{8}\left(\frac{k_\mathrm{B}T}{\pi m}\right)^{1/2}\frac{k_\mathrm{B}T}{P}\frac{f_\mathrm{D}}{\sigma^2\Omega^{(1,1)*}}, \tag{30}$$

where f_D is a higher-order correction factor, which can be defined as

$$f_\mathrm{D} = 1 + \frac{(6C^* - 5)^2}{8(2A^* + 5)}, \tag{31}$$

where A^* and C^* are given in Eqs. 27a and 27c, respectively. The binary diffusion coefficient (D_{12}), can also be obtained from the kinetic theory of polyatomic gases in terms of $\Omega_{12}^{(1,1)^*}$,

$$D_{12} = \frac{3}{8}\left[\left(\frac{m_1+m_2}{2m_1m_2}\right)\frac{k_\mathrm{B}T}{\pi}\right]^{1/2}\frac{k_\mathrm{B}T}{P}\,\frac{1+\Delta_{12}}{\sigma_{12}^2\Omega_{12}^{(1,1)^*}(T_{12}^*)}, \qquad (32)$$

where Δ_{12} is a higher-order correction term of the binary diffusion coefficient:

$$\Delta_{12} \approx 1.3(6C_{12}^* - 5)^2\,\frac{a_{12}x_{12}}{1+b_{12}x_{12}}, \qquad (33)$$

in which C_{12}^*, the ratio collision integrals, can be obtained from Eq. 27c and Table 4, and

$$a_{12} = \frac{\sqrt{2}}{8[1+1.8(m_2/m_1)]^2}\,\frac{\Omega_{12}^{(1,1)^*}(T_{12}^*)}{\Omega_{22}^{(2,2)^*}(T_{22}^*)}, \qquad (34a)$$

$$b_{12} = 10a_{12}[1+1.8(m_2/m_1)+3(m_2/m_1)^2]^{-1}, \qquad (34b)$$

in which $m_2/m_1 < 1$. Note that all units are in the SI system.

Table 5 contains the predicted viscosities and diffusion coefficients of low density from the inversion method. The absolute average percent deviations between the calculated and experimental values have also been included.

Conclusion

The effective intermolecular potential energy functions of the oxygen, nitrogen, and its mixture were calculated by the inversion technique. The potential energies for these systems, obtained by inversion of viscosity and second virial data, were used to evaluate improved collision integrals more accurately than is possible by the extended law of corresponding states. The improved collision integrals and their ratios can be used to calculate all of the transport coefficients within the precision of the experimental data. Our estimated accuracies are within 1% for the viscosity and 4% for the diffusion coefficient.

We are thankful to the Research Council of University of Tehran for their support of this work.

References

1 A. Boushehri, L. A. Viehland, and E. A. Mason, *Chem. Phys.*, **28**, 313 (1978).

2 H. Behnejad, A. Maghari, and M. Najafi, *J. Comput. Chem.*, **16**, 441 (1995).

3 A. Maghari and M. Najafi, *J. Phys. Soc. Jpn.*, **65**, 407 (1996).

4 A. Maghari and H. Behnejad, *Bull. Chem. Soc. Jpn.*, **71**, 1007 (1998).

5 B. Haghighi, A. Maghari, and M. Najafi, *J. Phys. Soc. Jpn.*, **67**, 3086 (1998).

6 A. Maghari, H. Behnejad, and F. Nematbakhsh, *J. Phys. Soc. Jpn.*, **68**, 2276 (1999).

7 P. E. Siska, J. M. Parson, T. P. Schafer, and Y. T. Lee, *J. Chem. Phys.*, **25**, 5762 (1970).

8 C. H. Chen, P. E. Siska, and Y. T. Lee, *J. Chem. Phys.*, **59**, 601 (1972).

9 A. L. J. Burgmans, J. M. Farrar, and Y. T. Lee, *J. Chem. Phys.*, **64**, 1345 (1976).

10 M. Keil, L. J. Danielson, and B. Buck, *J. Chem. Phys.*, **89**, 2866 (1988).

11 M. Welker, G. Steinbrunner, J. Solca, and H. Huber, *Chem. Phys.*, **213**, 253 (1996).

12 D. Gao, L. Chen, Z. Li, F. M. Tao, and Y. K. Pan, *Chem. Phys. Lett.*, **277**, 483 (1997).

13 S. Bock, E. Bich, and E. Vogel, *Chem. Phys.*, **257**, 147 (2000).

14 G. C. Maitland and E. B. Smith, *Mol. Phys.*, **22**, 861 (1971).

15 D. W. Gough, G. C. Maitland, and E. B. Smith, *Mol. Phys.*, **24**, 151 (1972).

16 D. W. Gough, E. B. Smith, and G. C. Maitland, *Mol. Phys.*, **25**, 1433 (1973).

17 G. C. Maitland and E. B. Smith, *J. Chem. Soc., Faraday Trans. 1*, **70**, 1191 (1974).

18 G. C. Maitland and E. B. Smith, *Mol. Phys.*, **24**, 1185 (1972).

19 S. Chapman and T. G. Cowling, "The Mathematical Theory of Non-Uniform Gases," 3rd ed, Cambridge University Press, London (1970).

20 G. C. Maitland, M. Rigby, E. B. Smith, and A. Wakeham, "Intermolecular Forces: Their Origins and Determination," Oxford University Press, Claredon (1998).

21 J. O. Hirschfelder, C. F. Curtiss, and R. B. Bird, "Molecular Theory of Gases and Liquids," Wiley, New York (1964).

22 A. Boushehri, J. Bzowski, J. Kestin, and E. A. Mason, *J. Phys. Chem. Ref. Data*, **16**, 445 (1987).

23 J. Bzowski, J. Kestin, E. A. Mason, and F. J. Uribe, *J. Phys. Chem. Ref. Data*, **19**, 1179 (1990).

24 L. A. Viehland, E. A. Mason, W. F. Morrison, and M. R. Flanney, *At. Data Nucl. Data Tables*, **16**, 495 (1975).

25 H. O'Hara and F. J. Smith, *J. Comput. Phys.*, **5**, 328 (1970).

26 H. O'Hara and F. J. Smith, *J. Comput. Phys.*, **22**, 47 (1971).

27 P. Clancy, D. W. Gough, G. P. Mathews, E. B. Smith, and G. C. Maithland, *Mol. Phys.*, **30**, 1397 (1975).

28 J. H. Dymond and E. B. Smith, "The Virial Coefficients of Pure Gases and Mixtures: A Critical Compilation," Oxford, Clarendon (1980).

29 K. R. Hall, *J. Chem. Eng. Data*, **39**, 873 (1994).

30 J. Kestin, H. E. Khalifa, S. T. Ro, and W. A. Wakeham, *Physica*, **88A**, 242 (1977).

31 J. M. Hellemans, J. Kestin, and S. T. Ro, *Physica*, **65**, 362 (1973).

32 B. A. Younglove, *J. Phys. Chem. Ref. Data*, **11**, 1 (1982).

33 R. A. Dawe and E. B. Smith, *J. Chem. Phys.*, **52**, 693 (1970).

34 F. A. Guevara, B. B. McInteer, and W. E. Wageman, *Phys. Fluids*, **12**, 2493 (1969).

35 A. Laesecke, R. Krauss, and K. Stephan, *J. Phys. Chem. Ref. Data*, **19**, 1089 (1990).

36 J. Kestin, S. T. Ro, and W. A. Wakeham, *Trans. Faraday Soc.*, **67**, 2308 (1971).

37 J. P. Matthews, C. M. S. R. Thomas, A. N. Dufty, and E. B. Smith, *J. Chem. Soc., Faraday Trans. 1*, **72**, 238 (1976).

38 A. A. Clifford, P. Gray, and A. C. Scott, *J. Chem. Soc., Faraday Trans. 1*, **71**, 875 (1975).

39 E. R. S. Winter, *Trans. Faraday Soc.*, **47**, 342 (1951).

40 H. F. Vugts, J. H. Boerboom, and J. Los, *Physica*, **50**, 593 (1970).

41 E. B. Winn, *Phys. Rev.*, **80**, 1024 (1950).

42 S. Weissman and E. A. Mason, *J. Chem. Phys.*, **37**, 1289 (1962).

43 J. Bohemen and J. H. Purnell, *J. Chem. Soc.*, **1961**, 360.